Science and Technology Indonesia
e-ISSN:2580-4391 *p*-ISSN:2580-4405
Vol. 9, No. 1, January 2024

Research Paper

High Performance of Ni-Al/magnetite Biochar for Methyl Orange Removal in Aqueous Solution

Neza Rahayu Palapa[1,2*], Zaqiya Artha Zahara[3], Risfidian Mohadi[2,4], Idha Royani[4], Aldes Lesbani[2,4]

[1]*Department of Chemistry, Faculty of Mathematics and Natural Science, Sriwijaya University, Ogan Ilir, South Sumatera, 30662, Indonesia*
[2]*Research Center of Inorganic Materials and Complexes, Universitas Sriwijaya, Palembang, South Sumatera, 30139, Indonesia*
[3]*Graduate School, Faculty of Mathematics and Natural Science, Sriwijaya University, Palembang, South Sumatera, 30139, Indonesia*
[4]*Master Program of Material Science, Graduate School Universitas Sriwijaya, Palembang, South Sumatera, 30139, Indonesia*
***Corresponding author**: nezarahayu@mipa.unsri.ac.id

Abstract
Elevated concentrations of dyes in water have a significant impact on both the aquatic ecosystem and human well-being. The adsorption approach, which is cost-effective and simple to use, was chosen for color treatment. The adsorbents used in this study were Modified Layered Double Hydroxides (LDHs) and Magnetite Biochar (MBC). To prepare the Ni-Al/MBC composites, a technique called coprecipitation and hydrothermal was employed. The successful preparation of these composites was confirmed through the use of characterization tests including X-Ray Diffraction (XRD), Fourier Transform-Infra Red (FT-IR), Brunauer Emmet Teller (BET), and Vibrating Sample Magnometer (VSM). The study focused on analyzing the kinetics, isotherms, and thermodynamics of adsorption in order to anticipate the mechanism of Methyl Orange (MO) adsorption. Additionally, the regeneration process was investigated to assess the adsorbent's ability for repeated usage. The percentage of Ni-Al/MBC adsorbed during the first to fifth regeneration cycles was 86.940%, 82.545%, 70.752%, 56.244%, and 34.503% respectively. The duration of contact was 70 minutes, as determined by the Pseudo Second Order (PSO) equation, with an adsorption rate of 0.0030 g/mg.min. The Langmuir equation indicated a maximum adsorption capacity of 45.455 mg/g.

Keywords
LDHs, Magnetite Biochar, Methyl Orange, Regeneration, Adsorption

Received: 8 October 2023, Accepted: 8 January 2024
https://doi.org/10.26554/sti.2024.9.1.156-166

1. INTRODUCTION

The discharge of dye contaminants, particularly the presence of methyl orange (MO) dye, into water sources has emerged as a pressing environmental issue (Ighalo et al., 2021). Methyl Orange is extensively utilized in diverse industries, such as textiles, printing, paints, (Purnomo and Mawaddah, 2020) and indicator pH (Haque et al., 2021) contributing to the growing burden of water pollution. Methyl Orange is a type of dye classified as an anionic colorant due to its chemical structure containing azo groups in Figure 1 (Wu et al., 2021). This categorization presents challenges in terms of its degradation, particularly under aerobic conditions, leading to its persistence in aquatic environments (Jemai et al., 2023). The resistance to aerobic degradation contributes to the bioaccumulation of methyl orange in water bodies (Mamat et al., 2018). Untreated methyl orange poses a significant threat to aquatic life and human health (Kishor et al., 2021). Addressing the deleterious effects of methyl orange contamination necessitates innovative and efficient treatment methods.

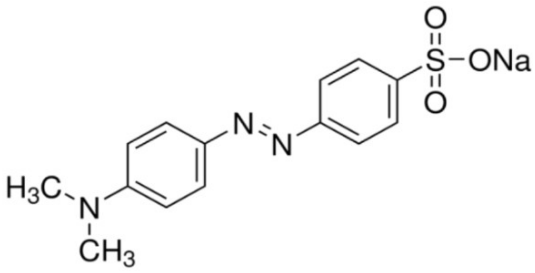

Figure 1. Chemical Structure of Methyl Orange (Mamat et al., 2018)

Numerous wastewater and dye treatment technologies have been developed, including photocatalysis (Regraguy et al., 2022), Advanced Oxidation Processes (AOPs) (Liu et al., 2022), biological treatment (Khan et al., 2022), ion exchange (Jia et al., 2020), coagulation-flocculation (Akter and Islam, 2022), and

adsorption (Alyasi et al., 2023). Adsorption has numerous benefits that make it a efficient approach for treating water and wastewater. These advantages encompass easy implementation with simple equipment needs, the lack of detrimental by-products, a substantial capacity for extracting contaminants from water solutions, and suitability for small-scale applications (Raji et al., 2022). Various adsorbents, such as activated carbon (El Maguana et al., 2020), zeolites (Radoor et al., 2021), and LDHs (Zaghloul et al., 2019), can be successfully utilized for eliminating dye contaminants.

Layered Double Hydroxides (LDHs) are a kind of two-dimensional materials that have similar properties to hydrotalcite. They have attracted significant attention due to their exceptional qualities and wide range of uses (Bini and Monteforte, 2018). Comprising layers resembling positively charged brucite, these materials are interspersed with anions that compensate for the charge, providing an exclusive foundation for customization and control through functionalization (Kameliya et al., 2023). LDH is represented by the chemical formula $[M^{2+}_{1-x}M^{3+}_{x}(OH)_2]x+[A_{x/n}]^{n-}mH_2O$, where M^{2+} (Zn^{2+}, Ca^{2+}, Mg^{2+}, Ni^{2+}, Cu^{2+}, Co^{2+}) and M^{3+} (Al^{3+}, Fe^{3+}, Cr^{3+}) are divalent and trivalent metal ions, respectively, and An^- is the interlayer anion (CO_3^{2-}, Cl^-, NO_3^-) (Zhang et al., 2021). Layered Double Hydroxides (LDHs) possess several advantages that render them appealing for various applications, including easy structural modification, particularly through anion intercalation within their positively charged layers, high chemical stability, and a substantial adsorption capacity (Abdallah et al., 2023). One of the drawbacks that need to be considered in LDHs is that the recovery and recycling of LDH may pose challenges because some recovery methods can lead to structural damage or reduce their performance (Yuliasari et al., 2022). The synthesis of Zn-Cr LDH has been carried out by Oktriyanti et al. (2019), with a maximum adsorption capacity increasing from 23.256 mg/g to 34.483 mg/g upon exchange with the Keggin ion to form $Zn-Cr-SiW_{12}O_{40}$ to remove Cr(VI).

The regeneration of adsorbents is essential to maintain their effectiveness over multiple usage cycles, thereby enhancing the economic and environmental viability of the adsorption process (Zahara et al., 2023). Research by Ahmad et al. (2023) the 2:1 magnetite humic acid adsorbent (MHA) applied to malachite green dye can adsorb up to 83.333 mg/g, and the adsorbent regeneration can occur for up to 3 cycles with the final adsorption percentage being 16.67%. The regeneration test results of Mg-Al/biochar adsorbent in Meili et al. (2019) study indicate that it can be utilized for up to 6 cycles in the removal of methylene blue dye, with an adsorption capacity decreasing from 70 to 40 mg/g. This modified adsorbent exhibits a maximum adsorption capacity reaching 406.47 mg/g. The incorporation of magnetite (Fe_3O_4) in the modification of LDH offers several advantages. The presence of magnetite enables more efficient separation and recovery of material mixtures. Magnetite particles can be directed or retrieved using a magnetic field, facilitating the recovery and recycling processes, thereby enhancing the adsorption performance for greater efficiency (Sajid and Ihsanullah, 2023). The modification of biochar with LDHs involves a recycling process, enabling sustainable utilization. The augmentation of adsorption capacity, facilitated by the additional adsorption sites and enhanced stability, contributes to optimizing the utilization of biochar (Juleanti et al., 2021).

Our research involves the modification of LDH with magnetite biochar using a coprecipitation method followed by hydrothermal. Prepared samples were characterized through X-Ray Diffraction (XRD), Fourier Transform-Infra Red (FT-IR), Brunauer Emmet Teller (BET), and Vibrating Sample Magnometer (VSM) analyses. The impact of the adsorbent regeneration process of adsorbents and influences the adsorption process of methyl orange, also the study explores various parameters affecting adsorption, including kinetics, isotherms, and thermodynamics.

2. EXPERIMENTAL SECTION

2.1 Materials and Instruments

The materials used included nickel nitrate hexahydrate $Ni(NO_3)_2.6H_2O$ (EMSURE® ACS, 290.81 g/mol), aluminum nitrate nonahydrate $Al(NO_3)_3.9H_2O$ (Sigma-Aldrich, 375.13 g/mol), iron (III) chloride $FeCl_3$ (Merck kGaA 162.20 g/mol), iron (II) sulfate $FeSO_4$ (Smart-Lab 278.01 g/mol), sodium carbonate Na_2CO_3 (EMSURE® ACS, 105.99 g/mol), biochar, hydrochloric acid HCl (MallinckrodtAR®, 37%), sodium hydroxide NaOH (EMSURE® ACS, 40 g/mol), methyl orange ($C_{14}H_{14}N_3NaO_3S$), Purite® water purification system from the ResearchCenter of Inorganic Materials and Complexes. The Rigaku Miniflex-6000 apparatus was used to conduct characterization utilizing multiple methods, including XRD analysis. The identification of FT-IR analysis was conducted using a Shimatdzu Prestige-21 spectrophotometer. The BET analysis was conducted using the N_2 adsorption-desorption apparatus manufactured by Quantachrome instruments. The user is doing a VSM analysis using the OXFORD VSM 1.2H 250-P2F model. The Biobase BK-UV 1800 PC UV-Vis spectrophotometer was used to measure absorbance values, with the maximum absorbance wavelength set at 460 nm.

2.2 Synthesis of Ni-Al Layered Double Hydroxide

The coprecipitation approach was used to synthesize Ni-Al LDH. At first, a 2 M sodium hydroxide (NaOH) solution with a volume of 50 mL was combined with a 0.3 M sodium carbonate (Na_2CO_3) solution with a volume of 100 mL. Afterwards, a 0.25 M solution of $Al(NO_3)_3.9H_2O$ (100 mL) and a 0.75 M solution of $Ni(NO_3)_2.6H_2O$ (100 mL) were slowly added to the mixture in order to attain a pH of 10. The pH adjustment was carried out using a 2 M solution of NaOH. The resultant mixture was agitated for a duration of 17 hours at a temperature of 80°C. Subsequently, the residue obtained was filtered, rinsed with purite® water, and then dried in an oven at a temperature of 100°C for a period of 24 hours.

2.3 Synthesis of Magnetite Biochar

A solution was prepared by dissolving 1 gram of $FeCl_3$ in 3 mL of Purite® water, while simultaneously dissolving 0.6 gram of $FeSO_4.7H_2O$ in 3 mL of Purite® water. The obtained solutions were combined and thereafter introduced to 1 gram of biochar. The combination was gently agitated at room temperature for a duration of 3 hours. Subsequently, a total of 3.5 mL of NH_3 solution was incrementally added dropwise to the mixture, which was then agitated at a temperature of 75°C for a duration of 30 minutes. The solution obtained was put into a hydrothermal stainless steel autoclave with a volume of 100 mL. The concoction was subjected to a temperature of 150°C and maintained at this level for a duration of 3 hours. The magnetite biochar's resulting solid product was isolated by filtering and then dehydrated in an oven at a temperature of 100°C.

2.4 Preparation of Ni-Al/magnetite biochar (Ni-Al/MBC) LDH composite

After incorporating 3 grams of biochar into the synthesis solution of Ni-Al LDH, the mixture was combined with a magnetite biochar solution and agitated at ambient temperature for a duration of 30 minutes. Subsequently, the mixture was put into a hydrothermal stainless autoclave and subjected to thermal treatment in an oven at a temperature of 150°C for a duration of 3 hours. The Ni-Al/magnetite biochar solution was filtered and washed with distilled water. It was then dried in an oven at a temperature of 100°C until a solid residue was formed. This residue was then crushed into powder.

2.5 Desorption and Regeneration Adsorbent Process

To initiate the regeneration procedure, 0.015 grams of substances were combined with 15 milliliters of methyl orange dye. The solution was agitated for a duration of 120 minutes. Following the agitation, the mixture was subjected to centrifugation, resulting in the separation of a filtrate and the residual adsorbent material. The UV-Vis spectrophotometer was used to measure the highest absorbance value of the filtrate. The residual adsorbed substance was subjected to drying, followed by the addition of 15 mL of Purite® water, and thereafter underwent desorption using an ultrasonic instrument. The desorbed material and the filtrate were separated. The UV-Vis spectrophotometer was used to measure the highest absorbance value of the filtrate. The material that was removed from the surface was then dried and then used for adsorption operations for a maximum of five cycles.

2.6 Adsorption Process of Methyl Orange

The adsorption kinetics method included introducing 0.015 gram of adsorbent into a 15 mL solution of methyl orange at a concentration of 30 mg/L. The agitation procedure was performed at several time intervals: 0, 5, 10, 20, 30, 50, 70, 90, 120, and 180 minutes. The isotherm and thermodynamic processes were approached in a similar manner, by considering the mass of the adsorbent and the volume of the adsorbate in the kinetics of adsorption. The isotherm and thermodynamic processes included concentration fluctuations of 5, 15, 30, 45, and 60 mg/L, together with temperature variations of 30, 40, 50, and 60°C. These variations were swirled for the duration established as optimal during the kinetics phase. The filtrate produced from the kinetics, isotherm, and thermodynamic processes was quantified using a UV-Vis spectrophotometer at the set peak wavelength. The adsorbed solute concentration was determined using Equation 1.

$$Q_e = \frac{(C_o - C_e)}{W} \times V \quad (1)$$

where concentration of adsorbed solute Q_e (mg/g), C_o is the initial concentration (mg/L), C_e is the remaining concentration (mg/L), W is the weight of the adsorbent (gram), and V is the volume of the adsorbate (liter).

3. RESULTS AND DISCUSSION

3.1 Characterization Results of X-ray Diffraction (XRD) Analysis

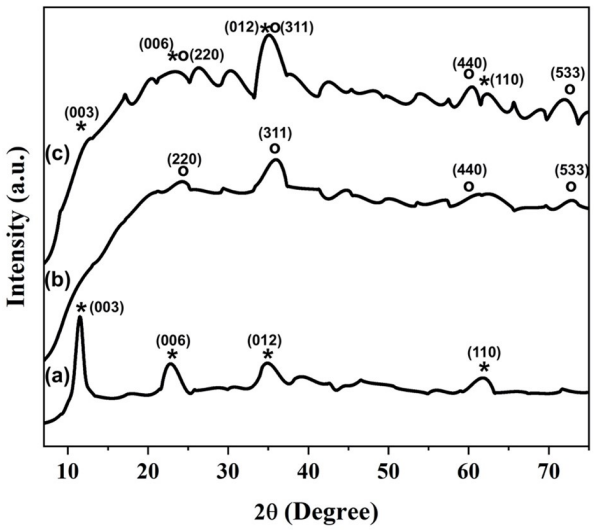

Figure 2. Diffractogram of Ni-Al LDH (a), Magnetite Biochar (b), and Ni-Al/MBC (c)

XRD analysis employs X-rays to ascertain the intermolecular interactions, which in turn produce precise spacing distances within the structure of the material. X-ray diffraction (XRD) analysis was conducted on Ni-Al LDH, magnetite biochar, and Ni-Al/magnetite biochar materials. The diffractogram findings are shown in Figure 2. The Ni-Al diffractogram exhibits characteristic LDH peaks, including peaks at 9-11° corresponding to layered structures and peaks at 60-61° corresponding to exchangeable anions. The diffraction pattern of the Ni-Al LDH sample shows peaks at angles of 11.57°, 22.91°, 35.04°, and 61.9°, corresponding to the crystallographic planes with Miller indices of 003, 006, 012, and 110, respectively. The

diffractogram of the Ni-Al material indicates the presence of both crystalline and amorphous structures, although with a modest degree of crystallinity. The synthesis successfully of Ni-Al LDH can be viewed from Utami et al. (2022) research by providing the peaks obtained from Ni-Al LDH in accordance with JCPDS data No.15-0087. The results of angle 2θ and miller index of magnetite biochar material are found in 23.8° (220); 35.79° (311); 61.1° (440); 72.8° (533). Consistent with the research Santhosh et al. (2020) of exhibits typical biochar angles of 22° and magnetite angles of 35° and 61° correlation with JCPDS No.82-1533. The Ni-Al/MBC composite has diffraction angles found in LDH and magnetite biochar, which are observed 12.07° (003), 23° (220), 35.3° (311), 60.30° (440) and 71.3° (533). The diffractogram results presented from the three adsorbents show that the synthesis of LDH, magnetite biochar, and preparation of modified LDH and composite were successfully carried out.

3.2 Characterization Results of Fourier Transform-Infra Red (FT-IR) Analysis

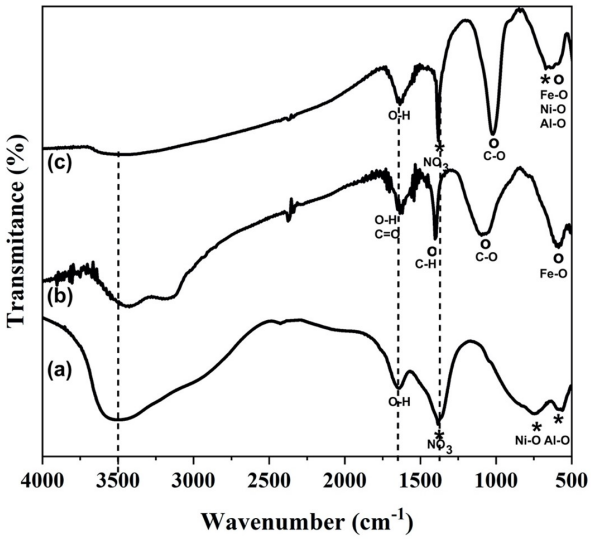

Figure 3. Spectrum IR of Ni-Al LDH (a), Magnetite Biochar (b), and Ni-Al/MBC (c)

FTIR analysis is used in the chemical bonding of a compound as shown in Figure 3 which produces vibrations by displaying the wavenumber of the three materials, Ni-Al LDH, magnetite biochar, and Ni-Al/MBC. Vibrations happen at the wavenumber for Ni-Al LDH indicating the presence of functional groups 3503 cm^{-1}, 1635 cm^{-1}, 1381 cm^{-1}, under 1000 cm^{-1} typical of LDH, consecutively O−H from water, O−H in the LDH bond, and M−O groups. The accomplishment of FT-IR characterization for Ni-Al LDH synthesis is related to the research conducted Manalu et al. (2023). The characteristic wavenumber of biochar magnetite material has been found in 3425 cm^{-1} indicate O−H, biochar represented in 1620 cm^{-1} presence C=O, 1404 cm^{-1} has a C−H, and C−O at 1095 cm^{-1}, magnetite found at 586 cm^{-1}. Similar research was found in Eltaweil et al. (2020) 1629 cm^{-1} functional group of =C=O, 1378 cm^{-1} indicate −COOH proves that the amount of oxygen content in biochar molecules and functional group of C−C, also Fe−O from Fe_3O_4 found at wavenumber 555 and 463 cm^{-1}. Characteristic Ni-Al/MBC composite wave numbers found in 3449 cm^{-1}; 2345 cm^{-1}; 1620 cm^{-1}; 1381 cm^{-1}; 1018 cm^{-1}, and 594 cm^{-1}, which is the combined wavenumber of LDH and magnetite biochar.

3.3 Regeneration and Desorption Process of Ni-Al, MBC, and Ni-Al/MBC

The regeneration process is applied to determine the adsorbent's potential for repeated adsorption. Related to XRD and FT-IR characterization to optimize the adsorbent regeneration process by presenting the stability of the structure as seen from before and after adsorption process. The use of ultrasonic devices in desorption processes with aqueous solvents employs ultrasonic waves by creating turbulences and microflows around the adsorbent, enabling the solvent water to access the adsorption sites. This can provide additional energy to increase the efficiency of the adsorption process (Daghooghi-Mobarakeh et al., 2020). Figure 4 clearly shows that the percentage of methyl orange adsorption with Ni-Al/MBC composite has not decreased much which is still above 30%. The percentage adsorbed using Ni-Al/MBC from the 1st to the 5th regeneration is as follows 86.940; 82,545; 70,752; 56,244; 34,503%. Significant reduction in % adsorbed occurs in Ni-Al LDH with percent adsorbed 64.397; 55.181; 36.866; 29.304; 14.424%. It is likely that the coating on LDH is exfoliated. Magnetite biochar also has a significant decrease in the fifth regeneration with a value of percent adsorption 70.069; 62.034; 58.135; 41.238; 27.767%, probably caused by adsorbed substances that are difficult to release thus reducing the percentage of adsorption.

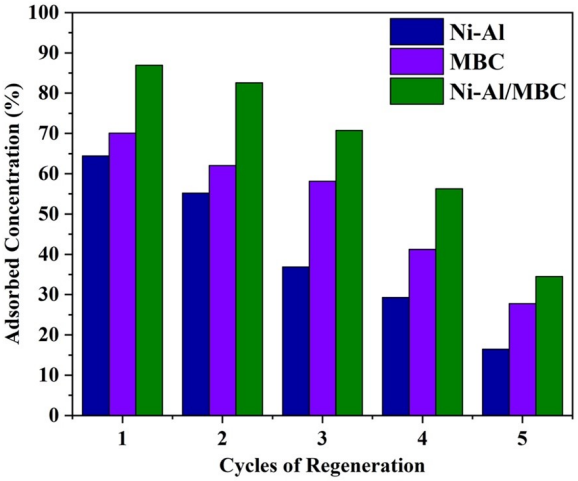

Figure 4. Percent Adsorbed Adsorbents Regeneration

Table 1. PFO and PSO Kinetics Model

Adsorbate	Kinetics Model	Parameter	Ni-Al LDH	MBC	Ni-Al/MBC
Methyl Orange	Pseudo-First Order	q_e exp (mg/g)	10.834	19.969	25.743
		q_e calc (mg/g)	4.4249	35.7520	19.7015
		k_1 (min^{-1})	0.0378	0.0509	0.0424
		R^2	0.8152	0.8389	0.9325
	Pseudo-Second Order	q_e exp (mg/g)	10.834	19.969	25.743
		q_e calc (mg/g)	13.4048	26.8097	27.8552
		k_2 (g/mg.min)	0.0024	0.0008	0.0030
		R^2	0.9053	0.9249	0.9953

Table 2. Langmuir and Freundlich Isotherm Model of Adsorption

Materials	Temperature (°C)	Adsorption Isotherm Model					
		Langmuir			Freundlich		
		Q_m	K_L	R^2	n	K_F	R^2
Ni-Al LDH	30	30.488	0.055	0.678	1.584	2.412	0.658
	40	29.412	0.074	0.7841	1.755	3.160	0.6408
	50	32.573	0.068	0.7663	1.665	3.104	0.6796
	60	31.949	0.085	0.8121	1.932	4.206	0.6058
MBC	30	43.668	0.027	0.9887	1.297	1.454	0.9882
	40	38.760	0.040	0.9933	1.434	2.029	0.9916
	50	36.232	0.058	0.9734	1.535	2.652	0.9598
	60	38.760	0.061	0.9769	1.506	2.844	0.951
Ni-Al/MBC	30	44.248	0.069	0.7914	1.549	3.796	0.7788
	40	45.045	0.076	0.8543	1.472	3.762	0.8424
	50	43.290	0.104	0.907	1.567	4.692	0.8322
	60	45.455	0.120	0.8954	1.631	5.648	0.7496

3.4 Characterization Results of Vibrating Sample Magnometer (VSM) Analysis

The adsorption capacity results, especially on thermodynamics, can be linked to the VSM characterization analysis by examining the efficiency with the regeneration without significantly reducing the adsorption capacity. VSM can provide information about the magnetic properties of materials used as adsorbents. Such knowledge can provide insight into the way magnetic materials interact with adsorbed substances and the way magnetic properties can influence the adsorption process in kinetics, isotherm, and thermodynamic. The magnetic saturation of MBC with a value of 13.04 emu/g in Figure 5(a) is greater than Ni-Al/MBC with value 8.35 emu/g in Figure 5(b). The magnetic fields of MBC and Ni-Al/MBC materials are 20.201 kOe and 20.201 kOe respectively. image results and magnetic values prove that MBC and Ni-Al/MBC are super-paramagnetism. The feature of super-paramagnetism is a hysterical non-circular curve that passes through the starting line or passes through point 0 in the magnetic field, and is easily attracted by an external magnetic field (Koo et al., 2019).

3.5 Kinetics Process of Adsorbents

Process kinetics involves setting the optimum time and rate of adsorption. The optimum time for the adsorption process methyl orange of Ni-Al LDH at 50 minute, magnetite biochar, and Ni-Al/MBC are respectively at 70 minute. Optimum time in the context of process kinetics refers to the time which gives the best results or highest efficiency in a reaction or process. The adsorption concentrations that have been obtained are plotted linearly using Microsoft Excel to determine Ni-Al LDH, magnetite biochar, and Ni-Al/MBC using the PFO (Pseudo First Order) and PSO (Pseudo Second Order) equations during the adsorption kinetics process as shown in Figure 6 and presented in Table 1. The analysis of the PFO and PSO equations is intended to understand how the solute is adsorbed on the adsorbent surface over time by looking at higher value of correlation coefficient (R^2). The determination of PFO and PSO calculation can also be decided by looking at the smaller adsorption rate value, and determining the calculated Q_e value which is closer to the experimental q_e value (Tran, 2023). Figure 6 illustrates that qe values are almost the same as t values (plot of q_e vs t). Ni-Al LDH, magnetite biochar,

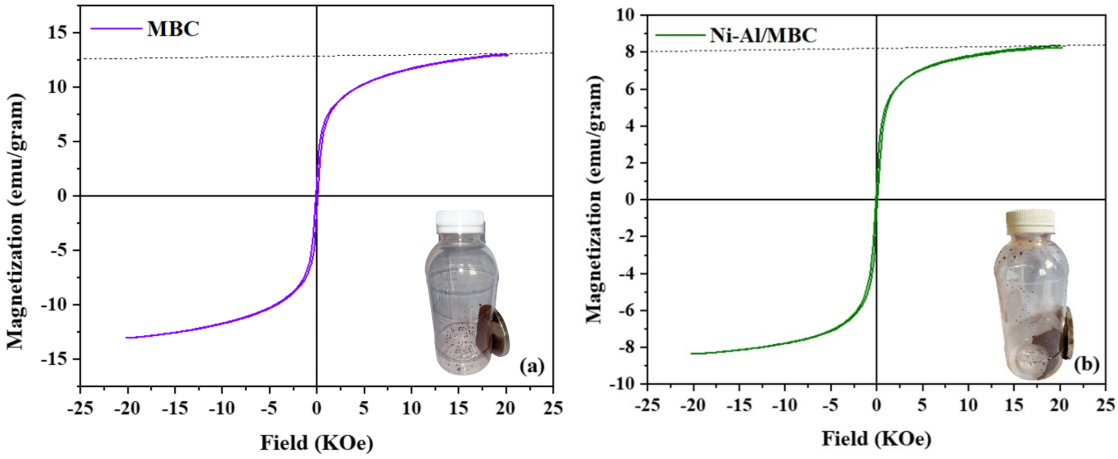

Figure 5. Magnetic Values and External Magnetic Force of MBC (a) and Ni-Al/MBC (b)

Table 3. Maximum Adsorption Capacities Methyl Orange of Other Research

Adsorbents	Q_{max} (mg/g)	References
Ocimum basilicum Linn Leaves (AC)	1.54	(Aruna Janani et al., 2023)
Poultry Manure Biochar (PMB)	20.8	(Ghani et al., 2022)
Hydroxyapatite	7.6	(Elsawy et al., 2022)
Magnetic Iron Oxide/Carbon nanocomposites	32.630	(Istratie et al., 2019)
Ni-Al LDH	31.949	This work
MBC	43.668	This work
Ni-Al/MBC	45.455	This work

and Ni-Al/MBC show that follows the PSO equation more closely with consecutive k_2 values of 0.0024; 0.0008; 0.0030 g/mg.min.

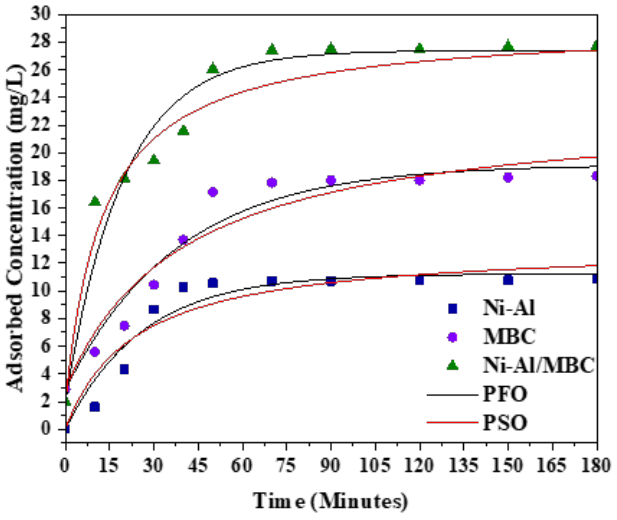

Figure 6. PFO and PSO Kinetic Equations for Each Materials

3.6 Isotherm and Thermodynamic Process of Adsorbents

Methyl orange adsorption process uses the effect of concentration and temperature to determine the isotherm and thermodynamic parameters of the Ni-Al LDH adsorbent, magnetite biochar, and Ni-Al/MBC composite using the optimum time that has been obtained. Figure 7 shows the effect of concentration and temperature of Ni-Al, MBC, and Ni-Al/MBC in adsorbing methyl orange. The increasing concentration of methyl orange dye solution is directly proportional to the increasing adsorption capacity. This is because at high temperatures the adsorbent and adsorbate molecules collide with each other and are reactive, so that it can facilitate the interaction in the processing of methyl orange dyes. Equilibrium occurs when the adsorbent's ability to adsorb dyes has reached an equilibrium phase, which is seen from the sloping graph or no significant increase.

Figure 7(a) shows the graph of the effect of concentration and temperature of Ni-Al LDH which has an experimental adsorption capacity of 23.529 mg/L. Magnetite biochar has a greater adsorption capacity in Figure 7(b) than precursor LDH which is 26.110 mg/L. Methyl orange can be adsorbed at 33.842 mg/L with the Ni-Al/magnetite biochar composite, which can be seen in Figure 7(c). The adsorption isotherm shows the Langmuir equation in Table 2 which shows for Ni-Al, MBC, Ni-Al/MBC, the adsorption process only occurs in one layer for adsorbate molecules bound to the adsorbent is

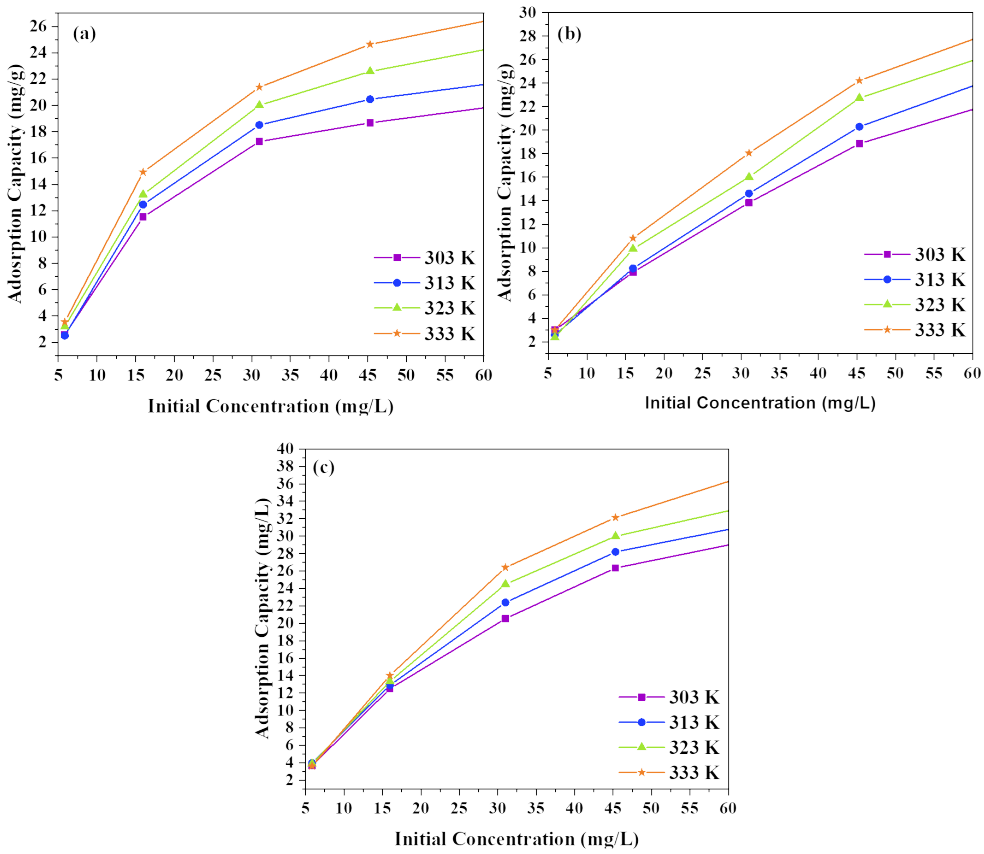

Figure 7. Effect Concentration and Temperature of Ni-Al (a) MBC (b) and Ni-Al/MBC (c)

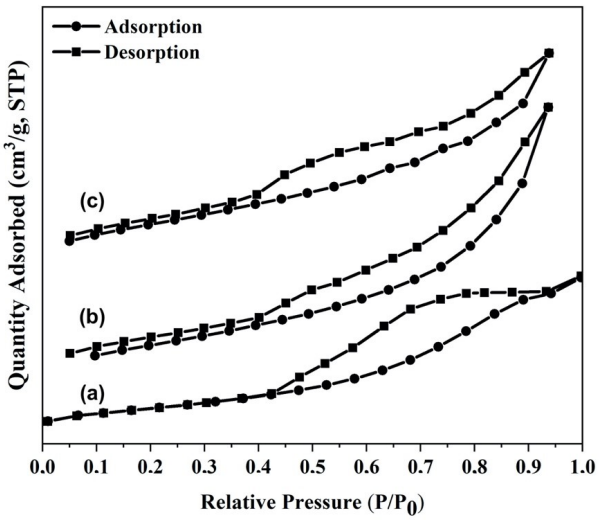

Figure 8. Graph Adsorption-Desorption of N_2 Gas from Ni-Al LDH (a), Magnetite Biochar (b), and Ni-Al/MBC (c)

more favourable and advantageous (Chen et al., 2017). The maximum adsorption capacities of other studies are shown in Table 3.

The spontaneity of the reaction on methyl orange dye is due to the enthalpy value of the reactants being higher than the enthalpy value of the products, and is supported by the process that continues until the equilibrium state. Table 4 shows the thermodynamic data of methyl orange dye on Ni-Al, MBC, and Ni-Al/MBC with negative (spontaneous) ΔG° values. Exceptions for Ni-Al LDH and magnetite biochar at concentrations of 45 and 60 mg/L with positive ΔG° values, so it needs influence from outside the system. Gibbs free energy changes or decreases in a reaction due to changes in pressure at each concentration of methyl orange dye involved in the adsorption reaction. The spontaneity of the reaction affects the degree of disorder, so that if the reaction occurs spontaneously, the system always goes towards homogeneous or the entropy value is increasingly positive and the system becomes more random (Bartel et al., 2018). Ni-Al, MBC, Ni-Al/MBC get a positive enthalpy value and a decrease in enthalpy value. This indicates that the adsorption process occurs endothermically. The thermodynamics shows physical adsorption with enthalpy less than 40 kJ/mol, indicating that the interaction between adsorbate and adsorbent is dominated by relatively weak Van

Table 4. Thermodynamics Data of Each Adsorbents

Co (mg/L)	T (°C)	ΔH (kJ/mol)			ΔS (J/mol.K)			ΔG (kJ/mol)		
		Ni-Al LDH	MBC	Ni-Al/MBC	Ni-Al LDH	MBC	Ni-Al/MBC	Ni-Al LDH	MBC	Ni-Al/MBC
5	30	12.271	15.568	16.035	0.039	0.052	0.057	0.517	-0.296	-1.286
	40							0.129	-0.820	-1.858
	50							-0.258	-1.343	-2.429
	60							-0.646	-1.867	-3.001
15	30	16.647	22.448	14.219	0.063	0.074	0.057	-2.381	0.072	-3.056
	40							-3.009	-0.666	-3.626
	50							-3.637	-1.405	-4.196
	60							-4.265	-2.143	-4.766
30	30	6.551	12.306	20.186	0.024	0.039	0.072	-0.592	0.606	-1.635
	40							-0.828	0.220	-2.356
	50							-1.064	-0.167	-3.076
	60							-1.299	-0.553	-3.796
45	30	8.079	10.105	9.358	0.024	0.030	0.034	0.890	0.878	-0.811
	40							0.653	0.574	-1.146
	50							0.416	0.269	-1.482
	60							0.179	-0.035	-1.817
60	30	7.558	7.987	8.573	0.019	0.022	0.027	1.827	1.445	0.263
	40							1.638	1.229	-0.011
	50							1.449	1.013	-0.285
	60							1.260	0.798	-0.560

Table 5. Textural Characteristics of the Adsorbents

Adsorbents	Surface Area (m^2/g)	Pore Volume (cm^3/g)	Pore Diameter (nm)
Ni/Al LDH	5.845	0.004	4.546
MBC	61.843	0.1279	4.1368
Ni-Al/MBC	127.310	0.1950	3.0638

der Waals forces, but the adsorbate is still locked on the adsorbent surface in a single layer in an orderly manner without the formation of strong chemical bonds (Tran et al., 2021).

3.7 Characterization Results of Brunauer Emmet Teller (BET) Analysis

BET analysis has been done to see the relationship of adsorption capacity derived from kinetics, isotherm and thermodynamics calculations with the results of surface area, pore volume, and pore diameter. However, it can be proven that if the surface area and pore volume of the adsorbent are large then the adsorbate is absorbed more, and vice versa, also the small pore diameter affects the process of fast adsorption rate. The use of N_2 gas in BET analysis resulted in the adsorption-desorption graph in Figure 8. Hysterical patterns generated from BET analysis refer to the IUPAC type IV classification which means the pore material isn't uniform, and the multilayer adsorption process at high relative pressures (Amri et al., 2023). Identification of the success of composite can be seen in Table 5 regarding surface area, pore volume, and pore diameter. The Ni-Al/MBC composite has a surface area with a high value 127.310 m^2/g and pore volume 0.1950 cm^3/g compared to its forming precursor, Ni-Al LDH with a value of 5.845 m^2/g, and magnetite biochar whose surface area is higher than LDH at a value 61.843 m^2/g.

4. CONCLUSION

Novel magnetic adsorbents with Ni-Al LDH modified magnetite biochar have been successfully synthesised using a simple two-step coprecipitation and hydrothermal technique with non-toxic and inexpensive precursors. Increase the carbon content of the magnetite significantly increased the removal

efficiency of methyl orange. XRD analysis show diffraction at 9-11° which are layered structures and peaks 60-61° which are exchangeable anions, also typical biochar angles of 22°, magnetite angles of 35° and 61°. FT-IR appeared wavenumber at 3503 cm^{-1}, 1635 cm^{-1}, 1381 cm^{-1}, under 1000 cm^{-1} typical of LDH, consecutively O−H from water, O−H in the LDH bond, NO_3^-, and M−O groups, biochar represented in 1620 cm^{-1} presence C=O, 1404 cm^{-1} has a C−H, and C−O at 1095 cm^{-1}, magnetite found Fe−O at 586 cm^{-1}. Higher specific surface area of Ni-Al, MBC, Ni-Al/MBC sequently 5.845; 61.843; 127.310 m^2/g. The amounts of MO adsorbed sharply increased within the first 50 Ni-Al and 70 minutes MBC, Ni-Al/MBC of the adsorption process. Both three-component solutions were effectively modelled by the pseudo-second order kinetic model. The two isothermal models, i.e. Langmuir, Freundlich, have been studied for the adsorption of a three component. Greater adsorption capacity maximum was observed for the adsorbents studied sequently 31.949; 43.668; 45.455 mg/g. Regeneration studies have shown that the Ni-Al/MBC adsorbent has great potential for reuse, using solutions of MO. The process is also simple and inexpensive. This makes it highly advantageous. Ni-Al/MBC composite display several promising advantages for potential commercial applications in the future.

5. ACKNOWLEDGMENT

The apparatus and materials utilised in this research were graciously supplied by the Laboratory located at the Research Centre of Inorganic Materials and Complexes, Sriwijaya University. For this, the authors are extremely appreciative.

REFERENCES

Abdallah, I. A., S. F. Hammad, A. Bedair, R. Abdelhameed, M. Locatelli, and F. R. Mansour (2023). Applications of Layered Double Hydroxides in Sample Preparation: A Review. *Microchemical Journal*; 108916

Ahmad, N., Z. A. Zahara, A. Wijaya, F. S. Arsyad, I. Royani, and A. Lesbani (2023). Fabrication and Characterization Fe_3O_4/Humic Acid for the Efficient Removal of Malachite Green. *Science and Technology Indonesia*, **8**(4); 617–625

Akter, S. and M. S. Islam (2022). Effect of Additional Fe^{2+} Salt on Electrocoagulation Process for the Degradation of Methyl Orange Dye: An Optimization and Kinetic Study. *Heliyon*, **8**(8); e10176

Alyasi, H., H. Mackey, and G. McKay (2023). Adsorption of Methyl Orange from Water Using Chitosan Bead-like Materials. *Molecules*, **28**(18); 6561

Amri, A., R. Rezonsi, N. Ahmad, T. Taher, N. R. Palapa, R. Mohadi, and A. Lesbani (2023). Biochar-Modified Layered Double Hydroxide for Highly Efficient on Phenol Adsorption. *Bulletin of Chemical Reaction Engineering & Catalysis*, **18**(3); 460–472

Aruna Janani, V., D. Gokul, N. Dhivya, A. Nesarani, K. Mukilan, A. Suresh Kumar, and M. Vignesh Kumar (2023). Optimization Studies on Methyl Orange (MO) Dye Adsorption using Activated Carbon Nanoadsorbent of *Ocimum basilicum* Linn Leaves. *Journal of Nanomaterials*, **2023**; 7969512

Bartel, C. J., S. L. Millican, A. M. Deml, J. R. Rumptz, W. Tumas, A. W. Weimer, S. Lany, V. Stevanović, C. B. Musgrave, and A. M. Holder (2018). Physical Descriptor for the Gibbs Energy of Inorganic Crystalline Solids and Temperature-Dependent Materials Chemistry. *Nature Communications*, **9**(1); 4168

Bini, M. and F. Monteforte (2018). Layered Double Hydroxides (LDHs): Versatile and Powerful Hosts for Different Applications. *Journal of Analytical and Pharmaceutical Research*, **7**(1); 00206

Chen, Q., Y. Tian, P. Li, C. Yan, Y. Pang, L. Zheng, H. Deng, W. Zhou, and X. Meng (2017). Study on Shale Adsorption Equation Based on Monolayer Adsorption, Multilayer Adsorption, and Capillary Condensation. *Journal of Chemistry*, **2017**; 1496463

Daghooghi-Mobarakeh, H., N. Campbell, W. K. Bertrand, P. G. Kumar, S. Tiwari, L. Wang, R. Wang, M. Miner, and P. E. Phelan (2020). Ultrasound-Assisted Regeneration of Zeolite/water Adsorption Pair. *Ultrasonics Sonochemistry*, **64**; 105042

El Maguana, Y., N. Elhadiri, M. Benchanaa, and R. Chikri (2020). Activated Carbon for Dyes Removal: Modeling and Understanding the Adsorption Process. *Journal of Chemistry*, **2020**; 1–9

Elsawy, H. A., Y. G. Emam, and D. A. Ali (2022). Kinetics and Isotherm Studies For Adsorption Of Methyl Orange Dye From Aqueous Solutions Using Hydroxyapatite. *Journal of Southwest Jiaotong University*, **57**(6); 1043–1052

Eltaweil, A., H. A. Mohamed, E. M. Abd El-Monaem, and G. El-Subruiti (2020). Mesoporous Magnetic Biochar Composite for Enhanced Adsorption of Malachite Green Dye: Characterization, Adsorption Kinetics, Thermodynamics and Isotherms. *Advanced Powder Technology*, **31**(3); 1253–1263

Ghani, U., W. Jiang, K. Hina, A. Idrees, M. Iqbal, M. Ibrahim, R. Saeed, M. K. Irshad, and I. Aslam (2022). Adsorption of Methyl Orange and Cr (VI) onto Poultry Manure-Derived Biochar from Aqueous Solution. *Frontiers in Environmental Science*, **10**; 887425

Haque, M. M., M. A. Haque, M. K. Mosharaf, and P. K. Marcus (2021). Decolorization, Degradation and Detoxification of Carcinogenic Sulfonated Azo Dye Methyl Orange by Newly Developed Biofilm Consortia. *Saudi Journal of Biological Sciences*, **28**(1); 793–804

Ighalo, J. O., A. G. Adeniyi, J. A. Adeniran, and S. Ogunniyi (2021). A Systematic Literature Analysis of the Nature and Regional Distribution of Water Pollution Sources in Nigeria. *Journal of Cleaner Production*, **283**; 124566

Istratie, R., M. Stoia, C. Păcurariu, and C. Locovei (2019). Single and Simultaneous Adsorption of Methyl Orange and Phenol onto Magnetic Iron Oxide/carbon Nanocomposites. *Arabian Journal of Chemistry*, **12**(8); 3704–3722

Jemai, R., M. A. Djebbi, S. Boubakri, H. Ben Rhaiem, and A. Ben Haj Amara (2023). Effective Removal of Methyl Orange Dyes Using an Adsorbent Prepared from Porous Starch Aerogel and Organoclay. *Colorants*, **2**(2); 209–229

Jia, Y., L. Ding, P. Ren, M. Zhong, J. Ma, and X. Fan (2020). Performances and Mechanism of Methyl Orange and Congo Red Adsorbed on the Magnetic Ion-Exchange Resin. *Journal of Chemical & Engineering Data*, **65**(2); 725–736

Juleanti, N., N. R. Palapa, T. Taher, N. Hidayati, B. I. Putri, and A. Lesbani (2021). The Capability of Biochar-Based CaAl and MgAl Composite Materials as Adsorbent for Removal Cr(VI) in Aqueous Solution. *Science and Technology Indonesia,*, **6**(3); 196–203

Kameliya, J., A. Verma, P. Dutta, C. Arora, S. Vyas, and R. S. Varma (2023). Layered Double Hydroxide Materials: A Review on Their Preparation, Characterization, and Applications. *Inorganics*, **11**(3); 121

Khan, A. U., M. Zahoor, M. U. Rehman, A. B. Shah, I. Zekker, F. A. Khan, R. Ullah, G. M. Albadrani, R. Bayram, and H. R. Mohamed (2022). Biological Mineralization of Methyl Orange by *Pseudomonas aeruginosa*. *Water*, **14**(10); 1551

Kishor, R., D. Purchase, G. D. Saratale, R. G. Saratale, L. F. R. Ferreira, M. Bilal, R. Chandra, and R. N. Bharagava (2021). Ecotoxicological and Health Concerns of Persistent Coloring Pollutants of Textile Industry Wastewater and Treatment Approaches for Environmental Safety. *Journal of Environmental Chemical Engineering*, **9**(2); 105012

Koo, K. N., A. F. Ismail, M. H. D. Othman, N. Bidin, and M. A. Rahman (2019). Preparation and Characterization of Superparamagnetic Magnetite (Fe_3O_4) Nanoparticles: A Short Review. *Malaysian Journal of Fundamental and Applied Sciences*, **15**(1); 23–31

Liu, X., Z. Chen, W. Du, P. Liu, L. Zhang, and F. Shi (2022). Treatment of Wastewater Containing Methyl Orange Dye by Fluidized Three Dimensional Electrochemical Oxidation Process Integrated with Chemical Oxidation and Adsorption. *Journal of Environmental Management*, **311**; 114775

Mamat, M., M. A. A. Abdullah, M. A. Kadir, A. M. Jaafar, and E. Kusrini (2018). Preparation of Layered Double Hydroxides with Different Divalent Metals for The Adsorption of Methyl Orange Dye from Aqueous Solutions. *Chemical Engineering*, **9**(6); 1103–1111

Manalu, R. N., Z. A. Zahara, and R. Mohadi (2023). Ni-Cr Layered Double Hydroxide/Microcrystalline Cellulose Composite as Adsorbents for Malachite Green Dye. *Indonesian Journal of Material Research*, **1**(2); 51–60

Meili, L., P. Lins, C. Zanta, J. Soletti, L. Ribeiro, C. Dornelas, T. Silva, and M. Vieira (2019). MgAl-LDH/biochar Composites for Methylene Blue Removal by Adsorption. *Applied Clay Science*, **168**; 11–20

Oktriyanti, M., N. R. Palapa, R. Mohadi, and A. Lesbani (2019). Modification Of Zn-Cr Layered Double Hydroxide With Keggin Ion. *Indonesian Journal of Environmental Management and Sustainability*, **3**(3); 93–99

Purnomo, A. S. and M. O. Mawaddah (2020). Biodecolorization of Methyl Orange by Mixed Cultures of Brown-Rot Fungus Daedalea Dickinsii and Bacterium *Pseudomonas aeruginosa*. *Biodiversitas Journal of Biological Diversity*, **21**(5); 2297–2302

Radoor, S., J. Karayil, A. Jayakumar, J. Parameswaranpillai, and S. Siengchin (2021). Efficient Removal of Methyl Orange from Aqueous Solution Using Mesoporous ZSM-5 Zeolite: Synthesis, Kinetics and Isotherm Studies. *Colloids and Surfaces A: Physicochemical and Engineering Aspects*, **611**; 125852

Raji, Y., A. Nadi, M. Rouway, S. Jamoudi Sbai, W. Yassine, A. Elmahbouby, O. Cherkaoui, and S. Zyade (2022). Efficient Adsorption of Methyl Orange on Nanoporous Carbon from Agricultural Wastes: Characterization, Kinetics, Thermodynamics, Regeneration and Adsorption Mechanism. *Journal of Composites Science*, **6**(12); 385

Regraguy, B., M. Rahmani, J. Mabrouki, F. Drhimer, I. Ellouzi, C. Mahmou, A. Dahchour, M. E. Mrabet, and S. E. Hajjaji (2022). Photocatalytic Degradation of Methyl Orange in the Presence of Nanoparticles $NiSO_4/TiO_2$. *Nanotechnology for Environmental Engineering*, **7**(1); 157–171

Sajid, M. and I. Ihsanullah (2023). Magnetic Layered Double Hydroxide-Based Composites As Sustainable Adsorbent Materials for Water Treatment Applications: Progress, Challenges, and Outlook. *Science of The Total Environment*, **880**; 163299

Santhosh, C., E. Daneshvar, K. M. Tripathi, P. Baltrėnas, T. Kim, E. Baltrėnaitė, and A. Bhatnagar (2020). Synthesis and Characterization of Magnetic Biochar Adsorbents for the Removal of Cr (VI) and Acid Orange 7 Dye from Aqueous Solution. *Environmental Science and Pollution Research*, **27**; 32874–32887

Tran, H. N. (2023). Applying Linear Forms of Pseudo-Second-Order Kinetic Model for Feasibly Identifying Errors in the Initial Periods of Time-Dependent Adsorption Datasets. *Water*, **15**(6); 1231

Tran, H. N., E. C. Lima, R. S. Juang, J. C. Bollinger, and H. P. Chao (2021). Thermodynamic Parameters of Liquid–Phase Adsorption Process Calculated from Different Equilibrium Constants Related to Adsorption Isotherms: A Comparison Study. *Journal of Environmental Chemical Engineering*, **9**(6); 106674

Utami, H. P., N. Ahmad, Z. A. Zahara, and M. R. Lesbani, A. (2022). Green Synthesis of Nickel Aluminum Layered Double Hydroxide using Chitosan as Template for Adsorption of Phenol. *Science and Technology Indonesia*, **7**(4); 530–535

Wu, L., X. Liu, G. Lv, R. Zhu, L. Tian, M. Liu, Y. Li, W. Rao, T. Liu, and L. Liao (2021). Study on the Adsorption Properties of Methyl Orange by Natural One-Dimensional Nano-Mineral Materials with Different Structures. *Scientific Reports*, **11**(1); 10640

Yuliasari, N., R. Mohadi, and A. Lesbani (2022). Modification of Pristine Layered Double Hydroxide to Form Metal Oxide Composites As an Anionic Dye Photodegradation Catalysts. *Communications in Science and Technology*, **7**(2); 168–174

Zaghloul, A., R. Benhiti, A. Soudani, M. Chiban, M. Zerbet, and F. Sinan (2019). Removal of Methyl Orange from Aqueous Solution Using Synthetic Clay Type MgAl-LDH: Characterization, Isotherm and Thermodynamic Studies. *Mediterranean Journal of Chemistry*, **9**(2); 155–163

Zahara, Z. A., I. Royani, N. R. Palapa, R. Mohadi, and A. Lesbani (2023). Treatment of Methylene Blue Using Ni-Al/Magnetite Biochar Layered Double Hydroxides Composite by Adsorption. *Bulletin of Chemical Reaction Engineering & Catalysis*, **18**(4); 659–674

Zhang, Y., H. Xu, and S. Lu (2021). Preparation and Application of Layered Double Hydroxide Nanosheets. *RSC Advances*, **11**(39); 24254–24281